

# Effects of Oxygen and Heat Treatment on the Mechanical Properties of Alpha and Beta Titanium Alloys

Z. LIU and G. WELSCH

Two alloys, Ti-6Al-2V and Ti-2Al-16V, simulating the alpha and beta phases of Ti-6Al-4V, respectively, were prepared with oxygen concentrations from 0.07 to 0.65 wt pct (0.20 to 1.83 at. pct). Their microstructure, deformation behavior, and strength were investigated with X-ray diffraction, microscopy, and mechanical tests to determine the effects of oxygen concentration and heat treatment. In both alloys the hardness increases in identical fashion with the square root of oxygen concentration. The alloys' strengths also depend on heat treatment, but in different ways. Whereas the alpha alloy is non-age-hardenable, the beta alloy's strength can be doubled by aging. The hardening effect of oxygen is generally unaffected by heat treatment, except for the alloys with the highest oxygen concentrations. During aging of the alpha a small amount of  $Ti_3Al$  can form, and slight age-hardening occurs. The ductility of the alpha alloy is little affected by aging. On the other hand, oxygen causes a change from good ductility at low oxygen concentration (0.07 wt pct) to total brittleness at 0.65 wt pct oxygen, independent of heat treatment. In the beta alloy there are complex phase transformations depending on heat treatment. Its deformation behavior varies from very ductile in solution-treated and quenched (STQ) condition to totally brittle in aged conditions. The aging embrittlement appears to be caused by alpha and some omega precipitation. Decoration of the beta grain boundaries with precipitates accounts for the intergranular brittle fracture. Oxygen, on the other hand, is not an embrittler, although it reduces the ductility of the beta alloy.

## I. INTRODUCTION

OXYGEN is the most important interstitial solute in titanium alloys because it strongly influences microstructural and mechanical properties. It is always present in significant concentration in commercial products. Most commercial titanium alloys contain concentrations between 0.10 and 0.20 wt pct oxygen which significantly affect the mechanical properties.<sup>1-4</sup> In fact, oxygen is often used as an alloying element to achieve desired strength levels or fatigue performance,<sup>5</sup> although such strengthening usually decreases the fracture toughness.<sup>6</sup>

The mechanical properties of alpha/beta titanium alloys have been the subject of much research of which only some is cited here.<sup>7-12</sup> Deformation of the alpha phase of Ti-6Al-4V was investigated as a function of oxygen concentration and aging temperature.<sup>13-19</sup> Investigations have also been made on other near-alpha titanium alloys.<sup>20-23</sup> In comparison, there is little information on the mechanical behavior of the minority beta phase in Ti-6Al-4V.<sup>16,17</sup> But there has been considerable interest in recent years in beta alloys of similar compositions.<sup>24-29</sup> The individual contributions of alpha and beta phase on the alloys' mechanical properties are not clear. There is a widely held belief that the alpha phase is responsible in a dominant way for the mechanical properties of  $\alpha + \beta$  Ti-6Al-4V alloys because of its large volume fraction. Also, the age-hardening of Ti-6Al-4V has been assumed to be controlled by microstructural changes in the alpha phase, based on experimental evidence of fine  $\alpha_2$  ( $Ti_3Al$ ) precipitation,<sup>13,30,31</sup> and based on explanations of oxygen ordering<sup>13,32</sup> and of decomposition of chemically homogeneous  $\alpha'$ -laths into  $\alpha + \beta$ . The precipitation of secondary alpha in beta phase regions during aging is also

well documented,<sup>13,33</sup> but in the Ti-6Al-4V alloy it has been given little attention because of the relatively small volume fraction of beta. A few have argued otherwise. For example, Lasalmonie *et al.*<sup>19</sup> concluded from microhardness experiments that not the alpha phase but the minority beta phase was principally responsible for age-hardening of Ti-6Al-4V alloy.

The present work was undertaken to obtain a better understanding of the relative roles of alpha and beta phases in two-phase titanium alloys, in particular Ti-6Al-4V alloy. The objective was to evaluate the microstructure and the mechanical behavior of alpha and beta separately. By preparing two alloys, simulating the compositions of alpha and beta phase, respectively, in Ti-6Al-4V the uncertainty about their individual contributions that arises from phase interaction in alpha/beta mixtures<sup>8,9</sup> is removed. The responses of alpha and beta alloys to heat treatment and to oxygen concentration can then be assessed individually and their respective behaviors can be compared with that of a two-phase Ti-6Al-4V alloy.

The equilibrium phase ratio of the Ti-6Al-4V alloy as a function of temperature and oxygen concentration is shown in Figure 1, according to Kahveci and Welsch.<sup>34</sup> With increasing oxygen concentration the phase ratio changes toward more alpha and the transus temperature  $T_t$  between alpha and beta is raised according to:<sup>34</sup>

$$T_t \text{ (}^\circ\text{C)} = 937 + 242.7[\text{O}] \quad [1]$$

where [O] is the oxygen concentration in weight percent. The chemical compositions of the phases vary with the phase ratio. These are indicated in Figure 1 by letters (A) through (C) for a Ti-6Al-4V alloy of less than 0.1 wt pct oxygen. The data are from Castro and Seraphin.<sup>30</sup> The elements Al and V partition into the alpha and beta phases, respectively. At 550  $^\circ\text{C}$ , for example, the vanadium concentration in the beta phase of an oxygen-lean alloy has increased to about 16 wt pct, and the aluminum concentration

Z. LIU, Graduate Research Assistant, and G. WELSCH, Associate Professor, are with the Department of Materials Science and Engineering, Case Western Reserve University, Cleveland, OH 44106.  
Manuscript submitted January 26, 1987.

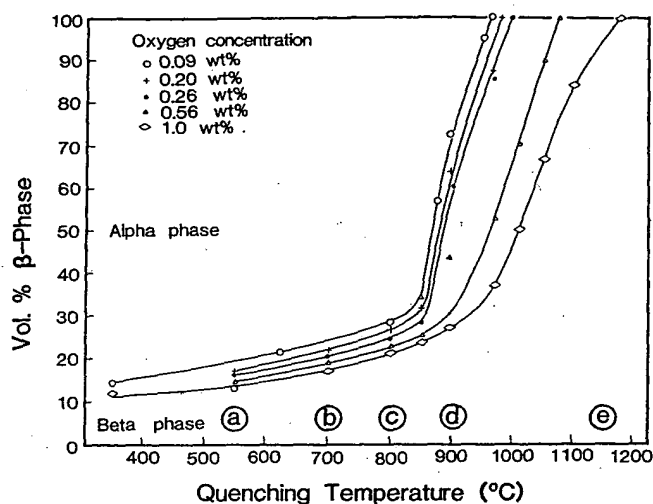


Fig. 1—Equilibrium volume fractions of alpha and beta phases in Ti-6Al-4V alloy as a function of temperature (from Kahveci and Welsch<sup>34</sup>). The compositions of the phases vary with volume ratio. The letters (a) through (e) indicate the beta compositions for an oxygen-lean Ti-6Al-4V alloy (from Castro and Seraphin<sup>35</sup>). (a) Ti-2Al-16V, (b) Ti-3Al-14V, (c) Ti-4Al-8V, (d) Ti-5Al-5V, and (e) Ti-6Al-4V.

has decreased to about 2 wt pct. Correspondingly, the alpha phase is enriched with aluminum to about 6.4 wt pct, and is depleted in vanadium to about 2.7 wt pct. Below 550 °C there are no significant concentration changes because diffusion is sluggish. With these considerations the compositions of the alloys to simulate the alpha and beta phases of Ti-6Al-4V were chosen as Ti-6Al-2V (alpha) and Ti-2Al-16V (beta). They were produced with a wide range of oxygen contents to encompass and exceed the concentrations encountered in commercial two-phase titanium alloys.

## II. EXPERIMENTAL

**Alloy Preparation:** The alloys were prepared with the consumable electrode arc melting technique.\* They were

\* in collaboration with RMI Corporation, Niles, Ohio.

cast into ingots, forged, and hot-rolled into 12 mm thick plates. An effort was made to keep identical compositions, except for systematic changes in oxygen concentration. The high oxygen concentrations were achieved by blending TiO<sub>2</sub> powder into the consumable electrode. The actual compositions of the alloys are shown in Tables I and II. Throughout the paper the concentrations are in weight percent, unless indicated otherwise.

To obtain standardized microstructural conditions all specimens were encapsulated in quartz tubes in vacuum of better than 10<sup>-3</sup> Pa, solution-heat-treated and water-quenched (STQ) to obtain single phase with uniform element distribution. Because of the strong influence of oxygen on the  $\alpha/\beta$  transus temperature of the alpha alloys, the solution treatments were chosen in relation to the transus temperature, and carried out at 40 degrees below the  $\alpha/\alpha + \beta$  transus temperatures, i.e., at 840 to 940 °C for the lowest and highest oxygen concentrations, respectively. The beta alloys were all quenched from 950 °C, irrespective of oxygen concentration. Finally, some specimens were

Table I. Chemical Composition of Alpha Alloy, Ti-6Al-2V (in Wt Pct)

Al	V	O	Fe	C	N	H
6.0	1.9	0.070	0.04	0.01	0.010	0.0051
6.0	2.0	0.202	0.03	0.02	0.015	0.0147
6.0	2.2	0.651	0.05	0.01	0.018	0.0092

Table II. Chemical Composition of Beta Alloy, Ti-2Al-16V (in Wt Pct)

Al	V	O	Fe	C	N	H
2.0	16.2	0.132	0.07	0.02	0.014	0.0094
2.0	15.4	0.204	0.06	0.01	0.018	0.0090
1.8	14.8	0.585	0.05	0.03	0.014	0.0046

aged at 350 °C or at 550 °C, again while encapsulated in vacuum. Bulk diffusion data indicate that at 350 °C oxygen has some diffusive mobility, while substitutional elements are frozen-in.<sup>35</sup> At 550 °C both interstitial and substitutional elements are mobile.

**X-ray Diffraction:** All specimens for X-ray diffraction studies were cut perpendicular to the rolling direction to minimize the texture effect.<sup>36</sup> The specimen sizes were 20 × 10 × 3 mm<sup>3</sup>. After heat treatment a 0.8 mm thick layer was ground off to eliminate possible surface layer contamination. Polished specimens were examined in a Philips powder diffractometer with nickel-filtered copper-K $\alpha$  monochromatic radiation at a scanning speed of 0.005 deg/sec.

**Microscopy:** Samples for optical microscopy were ground and mechanically polished with aluminum oxide powder, then etched in a solution of 5 pct HF, 10 pct HNO<sub>3</sub>, and 85 pct water. Samples for transmission electron microscopy were thinned by twin-jet electropolishing at -40 °C in a solution of perchloric acid, n-butyl alcohol, and methanol with the volume ratio 6:35:60.

**Hardness:** Samples for Vickers hardness testing were ground and polished with conventional metallographic methods. A Leitz Vickers tester was used for the measurements at indentation load of 2 kilograms. Ten measurements were taken from each sample.

**Tensile Tests:** The test samples were rectangular prisms with 6 × 3 mm<sup>2</sup> cross section and 25 mm gage length. A spindle-driven testing machine was used for the tests. The strain rate was approximately 3 × 10<sup>-4</sup>/second.

**Fracture Surface:** The fracture surfaces of tensile-ruptured specimens were examined in a scanning electron microscope (SEM) generating secondary electron image at an incident electron beam energy of 35 keV.

## III. RESULTS AND DISCUSSION

### A. Phases and Microstructures

1. **Alpha Alloy:** The X-ray diffraction data in Figure 2 reveal that the alpha alloy has hcp crystal structure for all oxygen concentrations and heat-treat conditions. No evidence of ordered phase was found by X-ray diffraction. In TEM, however, superdislocation pairs were found in the STQ alloy with 0.65 pct oxygen; see Figure 3(b). The latter suggests ordering of oxygen in the alpha alloy. We believe

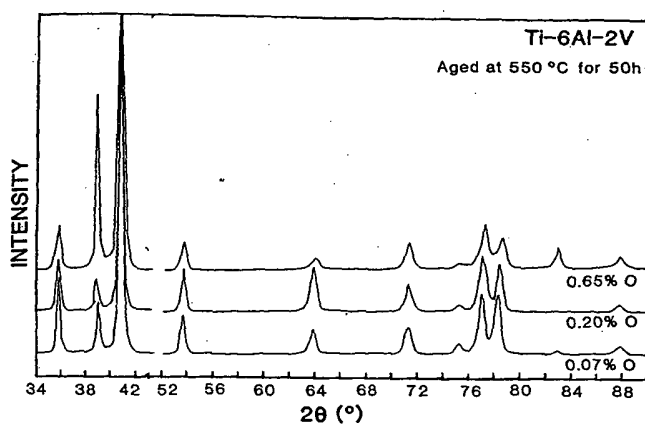
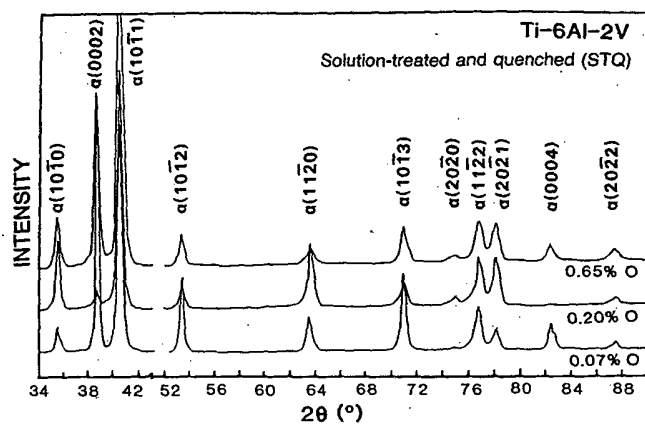
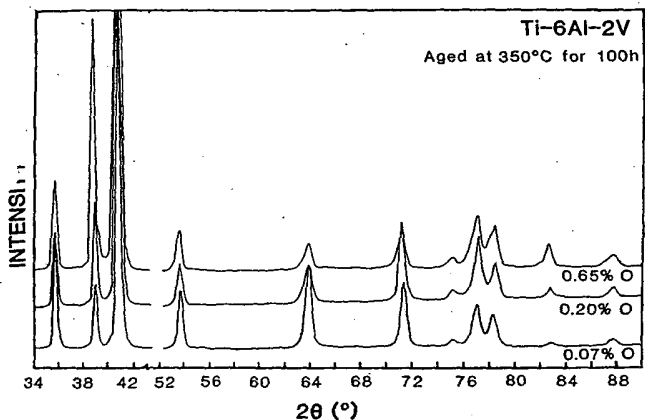


Fig. 2—X-ray diffraction spectra of alpha alloy Ti-6Al-2V with different oxygen contents and in different heat-treat conditions. No structure changes are detected.



that dislocation structure is a more sensitive indicator of ordering than diffraction because the diffraction intensity of the ordered sublattice may be too weak to be detected. Oxygen ordering is known to occur at concentrations of  $\geq 3$  wt pct (9 at. pct) in interstitial sites in every second plane parallel to the basal (0001) plane.<sup>37</sup> The question arises whether the superdislocation pairs in Figure 3(b) could possibly be due to ordering of aluminum. This question is justified because oxygen reduces the solubility of

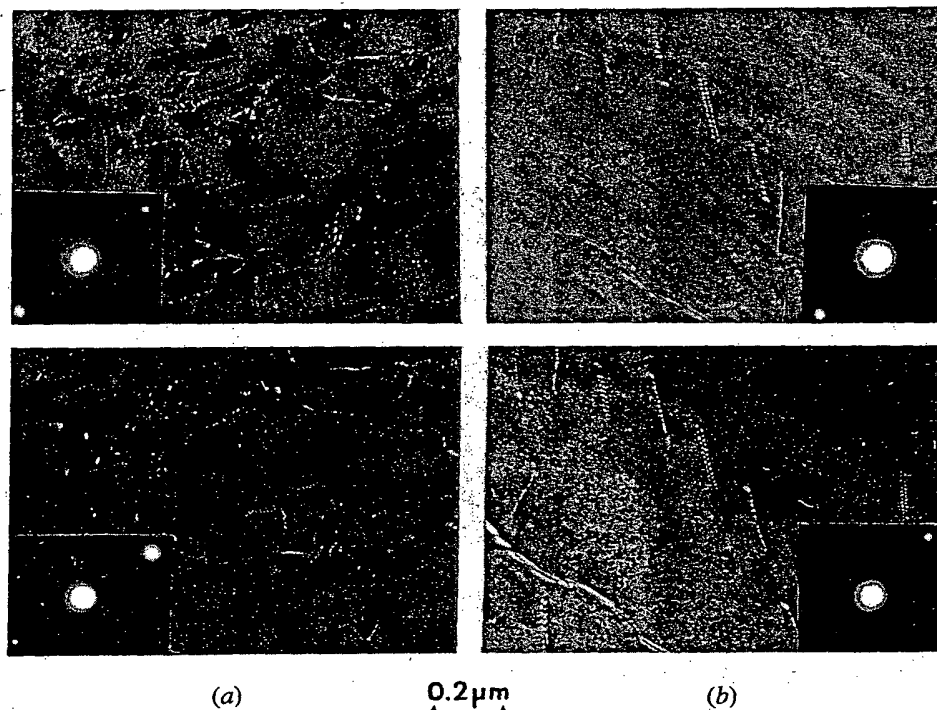


Fig. 3—Dislocations in alpha alloy of different oxygen concentrations. All are in the STQ condition. (a) 0.07 pct oxygen: random distribution of  $\bar{a}$ -dislocations, imaged with  $\bar{g} = [011]$ , top, and with  $\bar{g} = [01\bar{1}]$ , bottom. (b) 0.65 pct oxygen: superdislocation pairs,  $\bar{a}$ -type, imaged with  $\bar{g} = [101]$ , top, and with  $\bar{g} = [10\bar{1}]$ , bottom. The distance between dislocations of each pair does not change when the sense of  $\bar{g}$  is reversed. This fact indicates the dislocation pairs are superdislocations.

aluminum in titanium.<sup>38,39</sup> Also, Gehlen<sup>40</sup> had found enlarged octahedral holes in  $Ti_3Al$  making preferential uptake of (oxygen) interstitials in  $Ti_3Al$  likely. This can be interpreted that oxygen favors the formation of aluminum-ordering, the so-called  $\alpha_2$  phase ( $Ti_3Al$ ). Oxygen does in fact promote the precipitation of  $Ti_3Al$ , as will be shown below. However, superdislocation pairs were not found in samples in which there was diffraction evidence of  $Ti_3Al$  (see Figure 5), and therefore we conclude that they are evidence of oxygen-ordering in the alpha lattice.

The optical micrographs in Figure 4 show that the lamella structure of the alpha with 0.20 pct oxygen does not change during aging. The alloys with 0.07 and 0.65 pct oxygen behave similarly. However, weak electron diffraction spots of  $Ti_3Al$  were found after 550 °C aging (Figures 5(b) and (c)). The diffraction spot intensities were analyzed with a densitometer, and were normalized by setting the intensity of the alpha (0224) diffraction spot to unity. The normalized diffraction intensity of  $Ti_3Al$  (0111) increases from 0.08 to 0.22 as oxygen concentration increases from 0.07 to 0.65 pct. This is evidence that oxygen enhances the precipitation of  $Ti_3Al$ , in agreement with the findings of Nambodhiri *et al.*,<sup>38</sup> Truax and McMahon,<sup>39</sup> and Lim *et al.*<sup>41</sup>

2. *Beta Alloy*: In the STQ condition the beta alloys with 0.13 and 0.20 pct oxygen contain the orthorhombic  $\alpha''$  martensite<sup>42</sup> phase (Figure 6). The needle structure of the  $\alpha''$  phase is shown in Figures 7(a) and (b). However, in the alloy with high (0.59 wt pct) oxygen concentration the  $\alpha''$  phase was suppressed (Figures 6 and 7(c)), and the alloy's structure remained bcc after quenching. This result is surprising considering that oxygen is an alpha-stabilizing element. One would have assumed that oxygen would destabilize the bcc beta phase and promote the formation of alpha or of some intermediate phase between beta and alpha, such as  $\alpha''$ . But instead, oxygen suppresses  $\alpha''$  in favor of beta.

Aging at 350 °C for 100 hours causes most of the  $\alpha''$  phase to disappear from the STQ samples. The bcc beta phase is established, and weak reflections of alpha and omega precipitate phases are present in Figure 6. The two phases appear only in the alloys with low oxygen concentrations, and are suppressed in the alloy with 0.59 pct oxygen. Other investigators<sup>43,44</sup> also have found that during low temperature aging the formation of omega phase was slowed down as the oxygen content was increased from 0.065 pct to 0.15 pct, consistent with the present result.

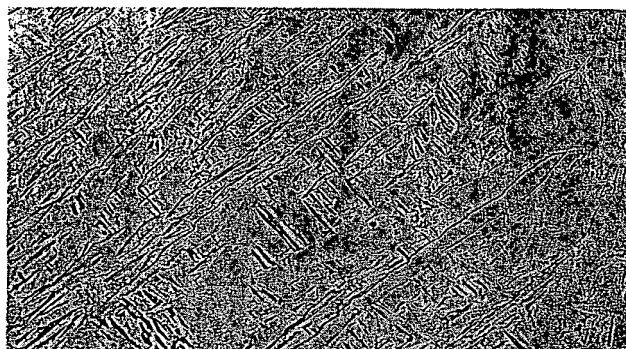
After aging at 550 °C for 50 hours, alpha phase has precipitated in the beta alloys. The alpha peaks are well defined in the X-ray diffraction spectra of Figure 6. Optical micrographs of the beta alloy, aged at 550 °C for 50 hours, are shown in Figure 8. Although the resolution is limited, continuous arrays of alpha precipitates are visible along the beta grain boundaries. They are confirmed by TEM in Figure 18.

#### B. Hardness as a Function of Oxygen Concentration and Heat-Treat Condition

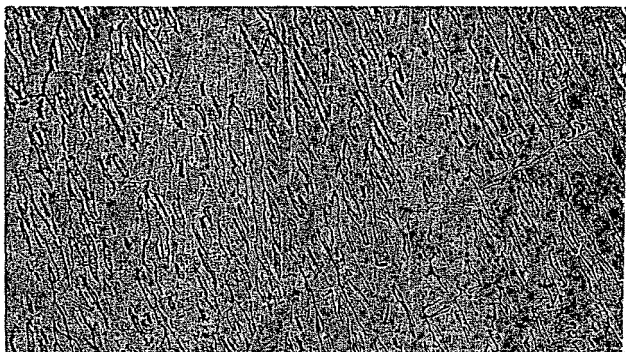
The hardening by oxygen of the alpha and beta alloys is shown in Figures 9(a), (b), and (c). Surprisingly, the oxygen's hardening effect is the same in alpha and beta alloys for all heat-treat conditions. The hardening is best described by a square root dependency on oxygen concentration [O]:



(a)



(b)



(c)

50  $\mu$ m

Fig. 4—Optical micrographs of alpha alloy with 0.20 pct oxygen. The microstructure is similar for all conditions: (a) STQ from 860 °C, (b) aged at 350 °C for 100 h, and (c) aged at 550 °C for 50 h.

$$H = H_T + b[O]^{1/2} \quad [2]$$

where  $H_T$  is the hardness of oxygen-free alloy, obtained by extrapolation of data to zero-oxygen concentration.  $b$  is a constant, and [O] is oxygen concentration in weight percent.  $H_T$  depends on heat treatment only. For the alpha alloy,  $H_T$  varies only slightly for different heat-treated conditions, but for the beta alloy it depends strongly on heat treatment. Table III shows values of  $H_T$ , and of the coefficient  $b$ , evaluated from linear regression analyses of the hardness data. The correlation coefficients  $r$  are near unity, which means the parabolic relationship between hardness and oxy-

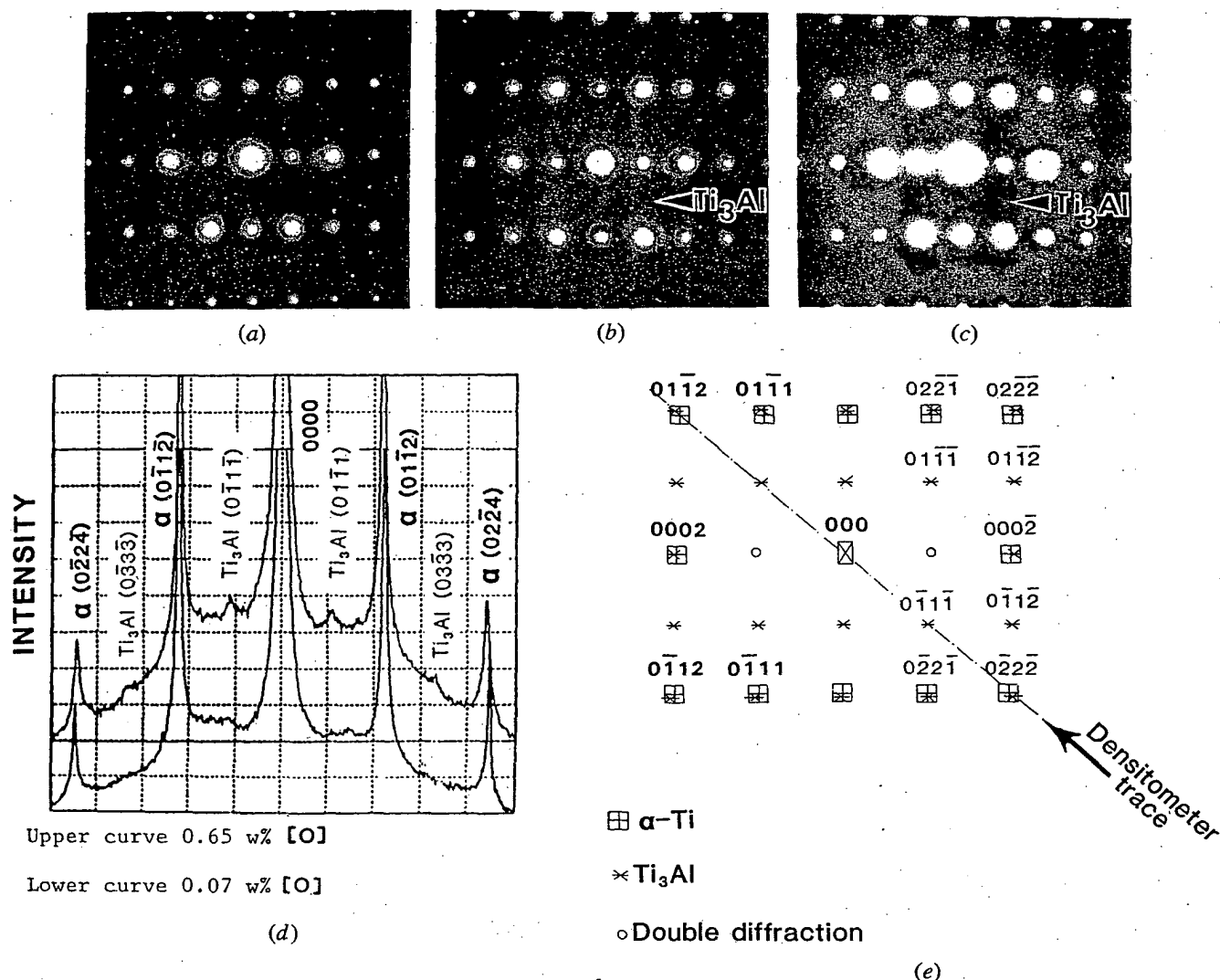


Fig. 5—Electron diffraction patterns of the alpha alloy of zone axis  $\bar{z}=[2\bar{1}\bar{1}0]$ . (a) There are no  $\text{Ti}_3\text{Al}$  reflections in the solution-treated and quenched condition. But after aging at 550 °C for 50 h, reflections of  $\text{Ti}_3\text{Al}$  precipitates appear, as shown in (b) and (c) for alloys with 0.07 and 0.65 wt pct [O]. The intensities of  $\text{Ti}_3\text{Al}$  increase with increasing oxygen concentration. This is evident from the densitometer traces of diffraction intensities in (d). The densitometer traces were taken along the path indicated by the dashed line in (e).

Table III. Values of the Coefficients  $H_T$  and  $b$  in Equation [2], Determined by Linear Regression of the Hardness Data, and Correlation Coefficient  $r$

	$H_T$ MPa	$b$ MPa (wt pct [O]) <sup>1/2</sup>	$r$
<b>Alpha Alloy Ti-6Al-2V</b>			
STQ from 840 to 940 °C	2160	2570	1.0000
Aged at 350 °C for 100 h	2390	2270	0.9970
Aged at 550 °C for 50 h	2620	1730	0.9938
<b>Beta Alloy Ti-2Al-16V</b>			
STQ from 950 °C	1300	2590	0.9890
Aged at 350 °C for 100 h	3750	2010	0.9988
Aged at 550 °C for 50 h	2420	1810	0.9830

gen concentration is closely followed in both alpha and beta alloys. Note, the quenched beta alloy is much softer than the alpha alloy, whereas after aging hardness can be considerably higher than that of alpha.

From the plots of hardness vs aging time in Figure 10, it is evident that the alpha alloy is not age-hardenable. The hardness values remain constant (i.e.,  $H_T = \text{const.}$ ) during aging. The 0.65 pct oxygen alloy is an exception. Its hardness decreases slightly during aging at 550 °C. The reason for the latter can only be speculated on. We believe that it may be due to reduction of the uniform oxygen concentration by segregation to boundaries or to  $\text{Ti}_3\text{Al}$  precipitates. Also, the scatter of the hardness data of the 0.65 pct oxygen alloy is much greater than that of the other alloys, with an average standard deviation of 170 MPa vs 82 MPa and 75 MPa for the alloys with 0.20 pct and 0.07 pct oxygen,

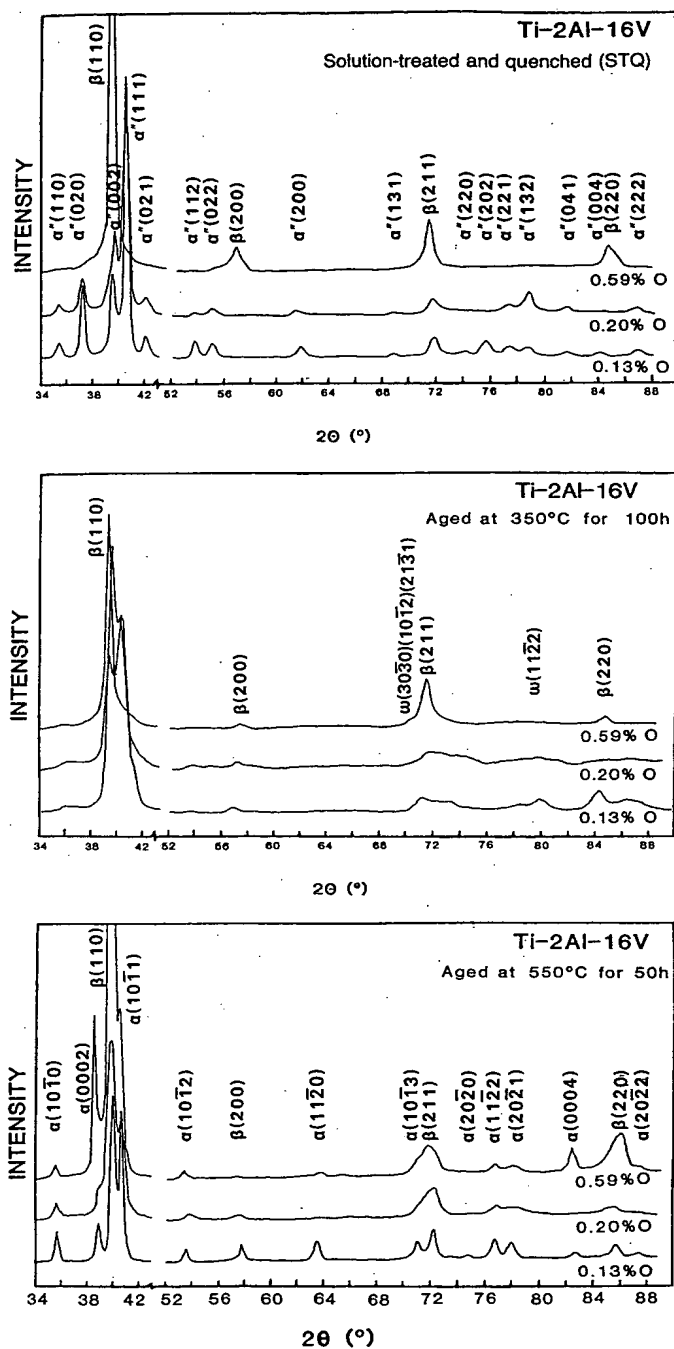
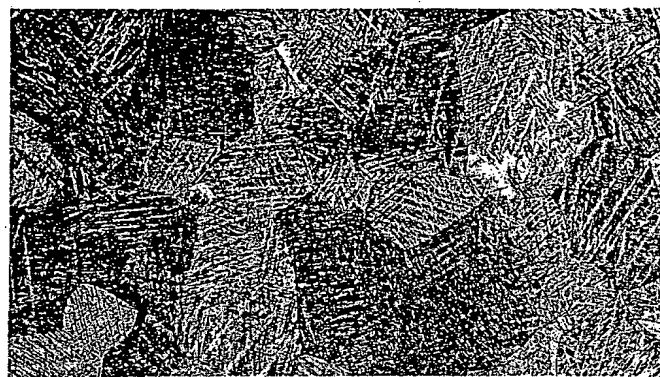


Fig. 6—X-ray diffraction spectra of beta alloy Ti-2Al-16V with different oxygen contents and in different heat-treatment conditions. In the STQ condition the alloys with 0.13 and 0.20 pct oxygen contain a large amount of  $\alpha''$  martensite phase. This phase is suppressed in the alloy with 0.59 pct oxygen. New precipitate peaks appear upon aging.

respectively. The increased scatter may be an indirect consequence of oxygen segregation.

The hardness of the beta alloy Ti-2Al-16V is strongly affected by heat treatment (Figure 11). During aging at 350 °C the hardness increases steadily with increasing aging time, and at 550 °C typical aging-overaging behavior is obtained.



(a)



(b)



(c)

400μm

Fig. 7—Optical micrographs of polished and etched beta alloy in the STQ condition. The alloys with 0.13 pct (a) and 0.20 pct (b) oxygen have  $\alpha''$  martensite, but the alloy with 0.59 pct oxygen (c) contains no martensite and has remained bcc beta.

The question of what influence oxygen has on age-hardening is of interest. In Figures 10 and 11 the hardness differential caused by oxygen is little affected by aging. For the alpha alloy, this has been taken as an indicator of no significant rearrangement of oxygen, with oxygen atoms assumed to be dispersed as a solid solution. However, the superdislocation pairs in Figure 3(b) indicate otherwise, namely that oxygen ordering does exist. The amount of order-hardening is not known. Conceivably, it is too insig-



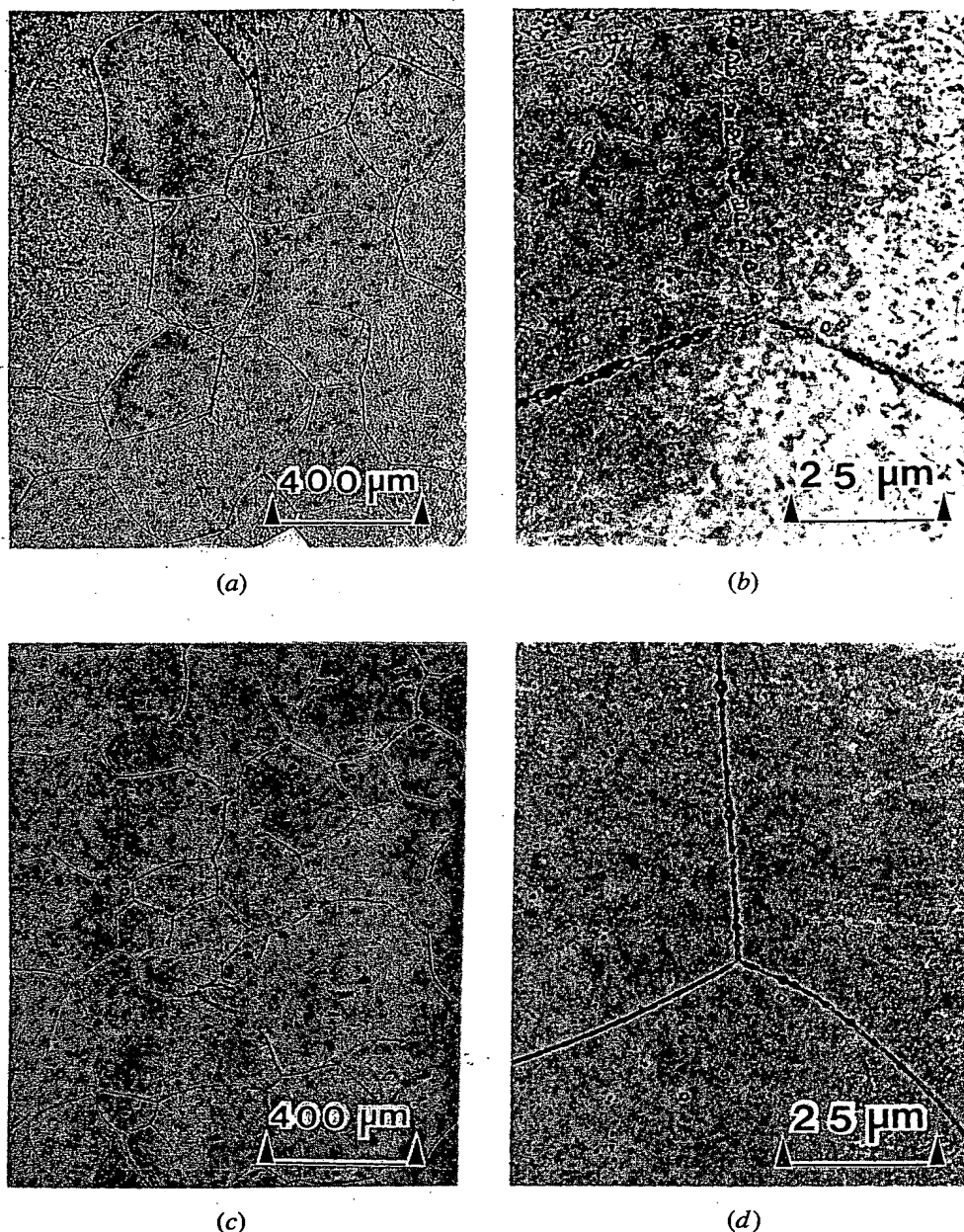


Fig. 8—Optical micrographs of the beta alloy aged at 550 °C for 50 h. The oxygen concentrations are (a) and (b) 0.13 pct, (c) and (d) 0.59 pct. Note that alpha precipitates have formed along the grain boundaries, as confirmed by TEM, Fig. 18.

nificant or indistinguishable from solution hardening to exert a measurable effect on the hardness.

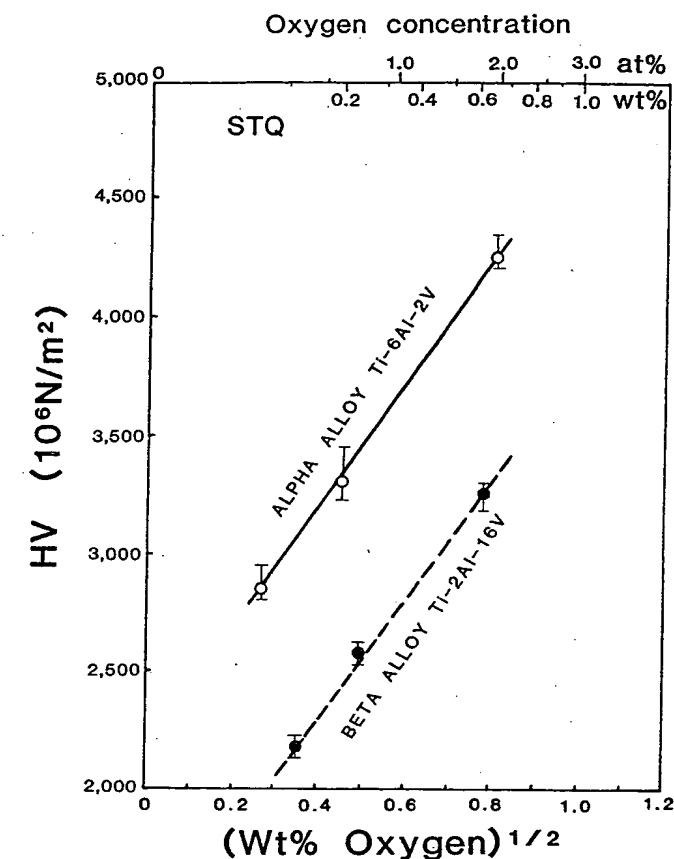
The strengthening of the aged beta alloy is due to precipitates and due to change of the crystal structure, as indicated by the X-ray data. The structure of the beta alloys with 0.13 and 0.20 pct oxygen changed from orthorhombic ( $\alpha''$ ) in the quenched condition to bcc during aging. With regard to the precipitates formed during aging, the coarsening of alpha precipitates at 550 °C accounts for the overage-softening after an initial hardening period. Age-hardening at 350 °C is more complicated because of the precipitation of very fine particles of alpha and omega.

### C. Hardness Comparisons

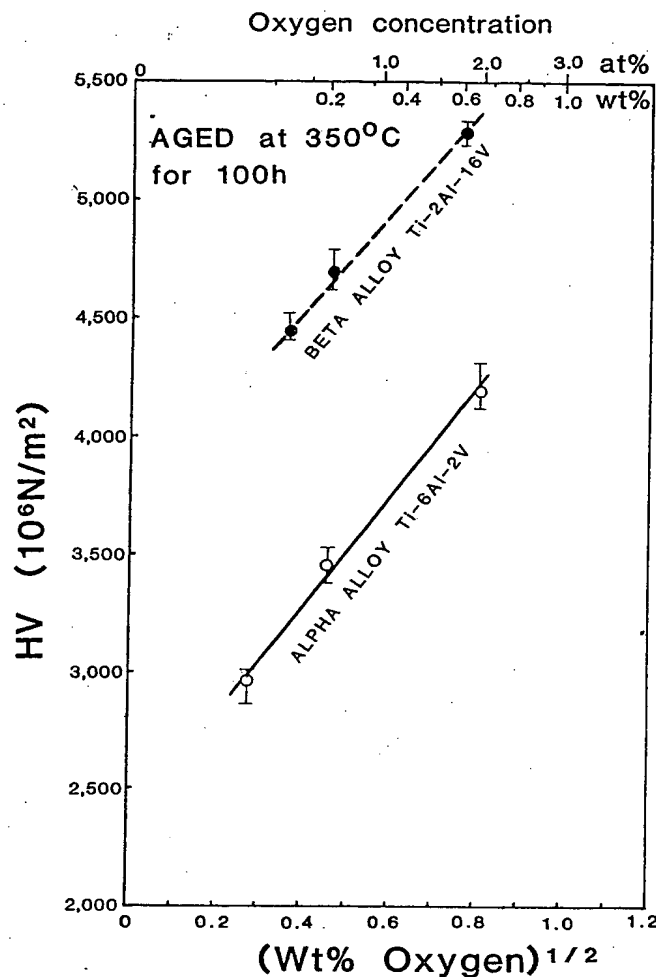
The hardness data of the separate alpha and beta alloys may be compared with those of the ( $\alpha + \beta$ ) Ti-6Al-4V alloy.<sup>45</sup> This is done in Figure 12 for several heat-treatment conditions of Ti-6Al-4V and for rule of mixture curves of the separate alloys.

$$H_{\text{mixture}} = f_{\alpha} \cdot H_{\alpha} + f_{\beta} \cdot H_{\beta} \quad [3]$$

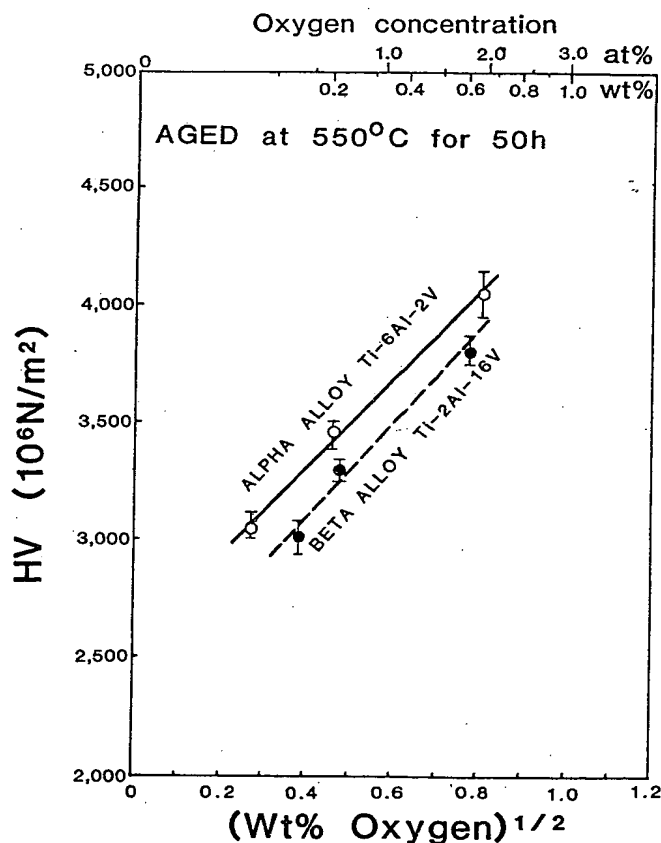
$f_{\alpha}$  and  $f_{\beta}$  are phase volume ratio fractions (see Figure 1).  $H_{\alpha}$  and  $H_{\beta}$  are the hardnesses of the separate alpha and beta alloys with the appropriate heat treatments (Figures 9(a),



(a)



(c)



(b)

Fig. 9—The hardness of the Ti-6Al-2V and Ti-2Al-16V alloys has a square root dependency on oxygen concentration. The same dependency is observed for different heat-treatment conditions: (a) solution-treated and water quenched (STQ) from 840 to 940 °C for the alpha alloy, and from 950 °C for the beta alloy. (b) Aged at 350 °C for 100 h, (c) aged at 550 °C for 50 h.

(b), and (c)). The comparisons can only be approximate, because the fixed compositions of the separate alpha (Ti-6Al-2V) and beta (Ti-2Al-16V) alloys cannot duplicate the varying phase compositions of Ti-6Al-4V (Figure 1), except for certain heat-treatment conditions. The 700 °C STQ and the long-time 550 °C-aged Ti-6Al-4V samples (and furnace-cooled samples in industrial applications) are reasonably well approximated by the separate, fixed alloy compositions, but for most other heat treatments the chemical compositions of the phases in Ti-6Al-4V are significantly different. With this in mind, the data in Figure 12 can be interpreted: From the slopes of the curves it is clear that the hardening potential of oxygen is the same in the two-phase and in the single phase alloys even when the substitutional element concentrations do not match. A comparison of the absolute values is not meaningful because of the varying chemical compositions of  $\alpha$  and  $\beta$  phases in Ti-6Al-4V (solution-strengthened) and because grain- or phase-boundaries and alloy morphology can make contributions to the hardness which were not studied here. There



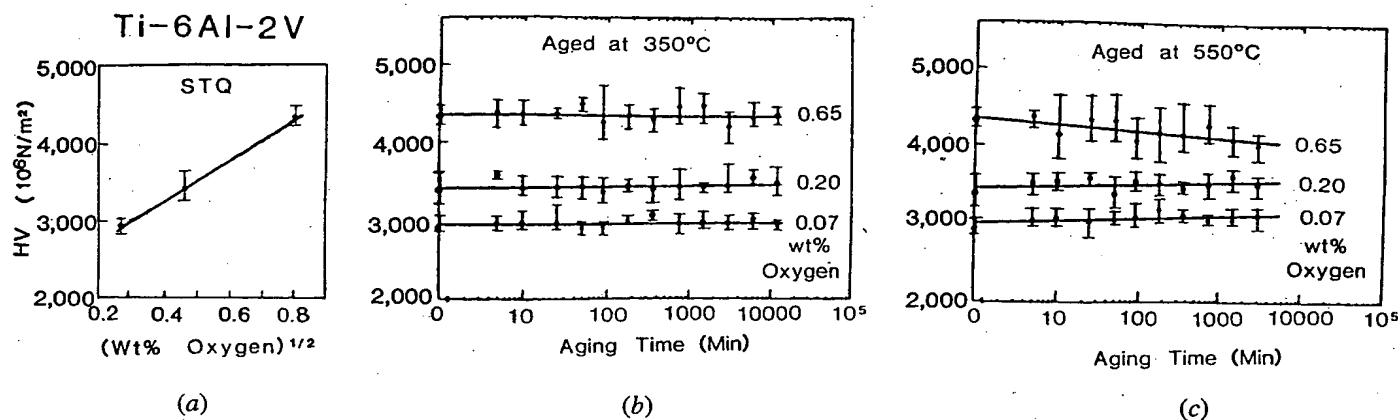


Fig. 10—(a) The alpha alloy Ti-6Al-2V is hardened by oxygen with a parabolic relation. (b) and (c) Aging does not produce additional hardening, irrespective of aging temperature and oxygen concentration. The hardening effect of oxygen remains essentially constant for all heat treatment conditions, except for the highest oxygen concentration of 0.65 wt pct the hardness decreases slightly with aging time.

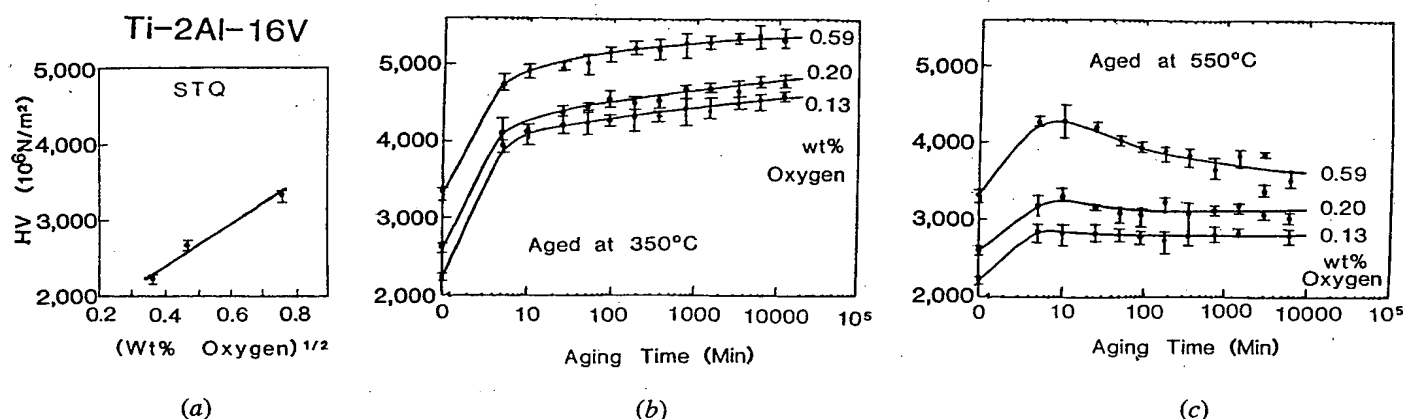


Fig. 11—(a) The beta alloy Ti-2Al-16V in STQ is hardened by oxygen with a parabolic relation. (b) and (c) Additional hardening is obtained from aging. The hardening effect of oxygen remains essentially constant for all heat treatments. Only for the highest oxygen concentration of 0.59 wt pct there is a slight deviation from this rule during aging at 550 °C, in that the oxygen effect is diminished.

is also a possibility that oxygen is partitioned between the phases in the two-phase alloy. The present results do not provide insight into oxygen partitioning.

In summary, oxygen hardens alpha and beta the same. The square-root dependency on concentration indicates solid solution strengthening as the mechanism. Ordering of oxygen in an interstitial sublattice does not change the parabolic dependency. With regard to the sensitivity to heat treatment, the alpha alloy is essentially not age-hardenable, whereas the beta alloy is significantly age-hardenable. From these results we conclude that the hardness increase of aged Ti-6Al-4V alloy is to a large degree controlled by the hardening of the beta phase instead of the alpha phase, in agreement with Lasalmonie *et al.*<sup>19</sup>

#### D. Overview of Hardening Mechanisms

The data provide a partial, but important picture of the hardening mechanisms contributing to the strength of ( $\alpha + \beta$ ) titanium alloys. The mechanisms are solid solution hardening by interstitial oxygen in both alpha and beta, oxygen order in alpha, and precipitation in beta. To put the

present work into perspective, an overview of all hardening mechanisms in alpha, beta, and in ( $\alpha + \beta$ ) alloys is given in Table IV. For some of the mechanisms reference has been made to data in this work. For other hardening mechanisms, reference has been made to literature.<sup>45-61</sup> In the simplest case the hardening mechanisms are additive.<sup>62</sup> There exist experimental data<sup>72</sup> to justify this assumption. But, if the strengthening mechanisms are interdependent, simple superposition does not take place. For example, work-hardening is very significant (designation *M* in Table IV) in alloys with yield strengths of less than 800 MPa, but not much work-hardening takes place when other hardening mechanisms have pushed the yield strength to a high level to begin with. When a mechanism produces only minor hardening, the designation *m* has been used in Table IV; see also the footnote at Table IV.

Metastable phases of beta are obtained after solution-treatment and quenching<sup>16</sup> of vanadium-containing Ti-alloys, as well as in alloys with other transition metals. They deform readily by stress-induced martensitic transformation,<sup>16,63</sup> thus making the alloys much softer than would be expected from solid solution-hardening by the alloy ele-

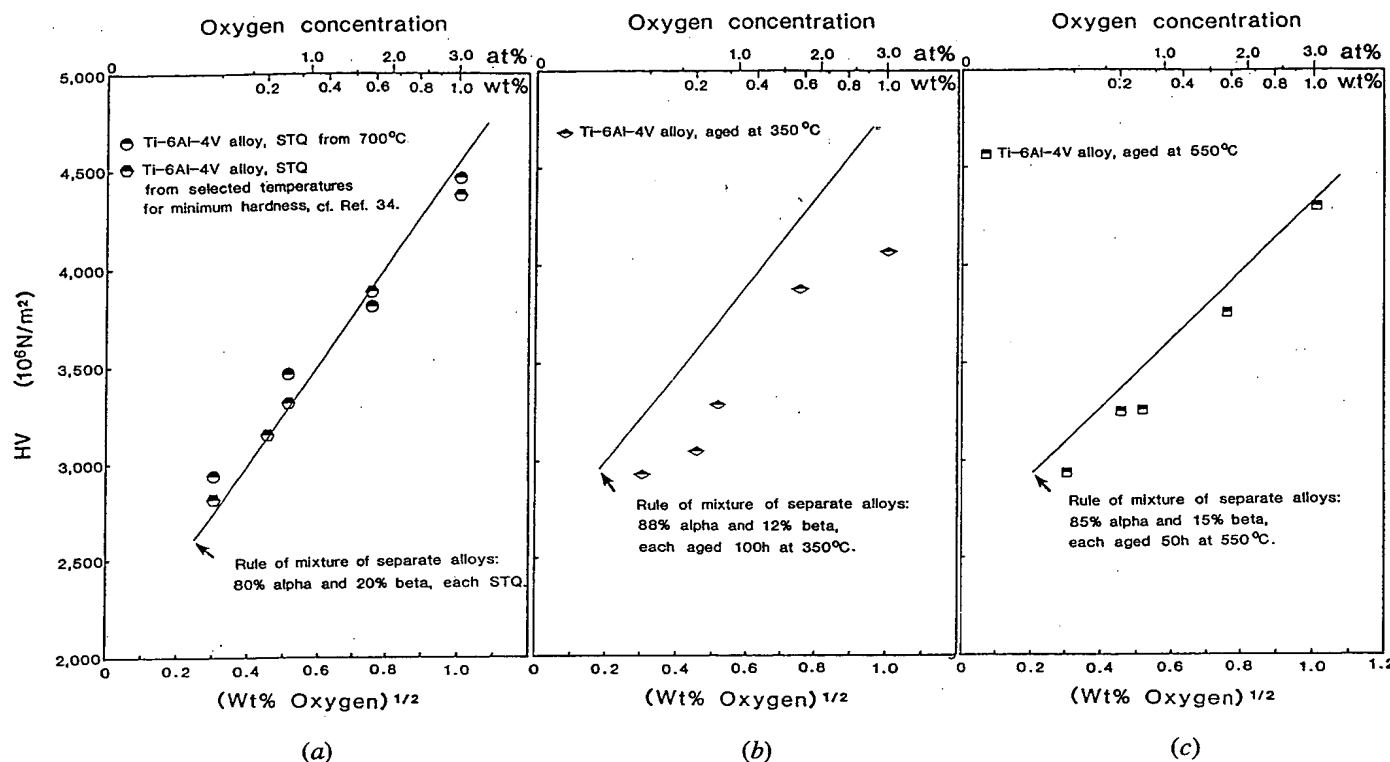


Fig. 12—Comparison of hardness data of two-phase, lamellar Ti-6Al-4V with rule of mixture curves determined from separate alpha (Ti-6Al-2V) and beta (Ti-2Al-16V) alloys. The volume fractions for the mixtures are based on Fig. 1. The dependencies on oxygen concentration are shown for (a) solution-treated and quenched (STQ) conditions, (b) 350 °C-aged condition, and (c) 550 °C-aged condition.

ments. Mechanical softening due to phase metastability is a frequently encountered phenomenon<sup>64</sup> in metal alloy and in ceramic systems.

The strengthening potential of substitutional alloys has been amply documented in alpha-titanium,<sup>1,2,48,49</sup> but only a few references exist for beta-titanium, presumably because of the difficulty of distinguishing the effects of solid-solution-hardening and metastable-phase-softening.

The solid-solution-hardening by interstitial oxygen has been addressed in this paper and in some previous references. It is clear that relatively modest oxygen concentrations, compared to substitutional alloy concentrations, make major contributions to the alloys' hardnesses. There is also the superdislocation evidence for oxygen-order in alpha-titanium (Figure 3). However, at present, we are unable to say what contribution such ordering might make to the hardness. The superdislocation pairs have a-character, and can slip in principle on pyramidal, prism, and basal planes. However, if the oxygen order suppresses  $\bar{c}$ -component slip,<sup>65</sup> this would explain the severe embrittlement of alpha-titanium by oxygen. This possibility is the subject of further investigation.<sup>45,66</sup>

Precipitation-hardening is another major contributor to the strength of beta- and of  $(\alpha + \beta)$  alloys. It is easily controlled by heat treatment. The hardening of alpha-titanium by  $Ti_3Al$  precipitates appears to be of minor significance (see 550 °C-aged samples in Figures 10 and 13), but the hardening of the beta phase by alpha, and in some instances by omega precipitates, is very significant.

Hardening due to refined grain size, lamella size, or lamella packet size must be mentioned. The materials in the

present study were all coarse-grained or coarse-lamellar with alpha-lamella widths of 10 to 50  $\mu m$ , lamella packets of 500 to over 1000  $\mu m$ , and beta grain size of 200 to 500  $\mu m$ . It is clear that there is much room for Hall-Petch hardening by grain refinement.<sup>56,57,59</sup> There exists a large body of literature on thermal-mechanical processing to obtain desired lamella or equiaxed microstructures<sup>50,58,67-72</sup> for optimization not only of strength and ductility but of fracture toughness and fatigue resistance as well.<sup>55,59,73-77</sup> Broadly speaking, it appears that Hall-Petch relations are obeyed for boundaries across which there is a major change of slip orientation, such as grain boundaries or phase boundaries in equiaxed alloys. Also, lamella packet boundaries fit this criterion, whereas lamella boundaries and the width of lamellae inside a packet seem to play a subjugated role because packets often behave like a single crystal.

The strain-rate ( $\dot{\epsilon}_p$ ) effect on the strength of alpha and (alpha + beta) titanium alloys has been investigated by Monteiro *et al.*<sup>60</sup> and Meyer<sup>61</sup> covering the range of  $10^{-5}$  to  $10^4$   $s^{-1}$ . The hardening is 30 to 50 MPa per order of magnitude increase of  $\dot{\epsilon}_p$ , but is significantly higher at very high strain rates of the order of  $10^3$   $s^{-1}$  and up.<sup>61</sup> In the present investigation the strain rates were much lower, order of  $10^{-4}$   $s^{-1}$  in tensile tests. The strain rates in micro-hardness indentations are difficult to estimate but are most certainly below  $10^{-1}$   $s^{-1}$ .

### E. Tensile Properties

1. *Alpha Alloy:* The tensile stress-strain curves of specimens with 0.07 pct oxygen are shown in Figure 13(a). They

Table IV. Overview of Mechanisms Contributing to the Hardness of Alpha, Beta, and Alpha + Beta Titanium Alloys at Room Temperature

Contribution to Hardness	Alpha Alloy	Beta Alloy	Alpha + Beta Alloy
$H_i$ Intrinsic lattice flow stress	m, Refs. 1, 2	no data	(*) Ref. 8
$H_{wh}$ Working hardening	m/M, Fig. 13, this work. Refs. 2, 46	m/M, Fig. 15, this work. Ref. 17	m/M, Refs. 13, 14
$H_{mp}$ Metastable phase	—	M, softening due to metastable $\beta$ or $\alpha''$ , Fig. 15 and Refs. 15 to 18	M, softening due to metastable $\beta$ or $\alpha''$ , Refs. 15 to 18, 47
$H_{ss,s}$ Solid solution hardening due to substitutional alloy elements	M, Refs. 1, 2, 48 to 50	(**) Ref. 51	M
$H_{ss,i}$ Solid solution hardening due to interstitial elements	M, Figs. 9, 10, 13, this work. Refs. 2, 52	M, Figs. 9, 11, 15, this work.	M, Fig. 12, this work. Refs. 14, 17
$H_{oi}$ Ordering of interstitial (oxygen) atoms	(m/M)?, Fig. 3, this work	no data	no data
$H_{ppt}$ Precipitation hardening: -Ti <sub>3</sub> Al in alpha → - $\alpha$ , $\omega$ in beta →	m, Figs. 5, 10, 13, this work. Refs. 13, 14, 53, 54	no data  M, Figs. 6, 8, 11, 12, 15, 18, this work. Ref. 46	M, Refs. 13, 14, 28, 33, 46
$H_b$ Boundary hardening (Hall-Petch) -Grain boundaries -Lamella packet boundaries -Lamella boundaries within a packet. (Phases are Burgers-orientation related) -Phase boundaries in equiaxed two-phase alloys (do not have Burgers-orientation relation)	M, Refs. 56, 57	Ref. 58	M,   Ref. 59
$H_{sr}$ Strain rate effect	Ref. 60	no data	Ref. 61

M: Major contribution, e.g., Vickers hardness changes of over 600 MPa, or yield strength changes of over 200 MPa.

m: Minor contribution, e.g., Vickers hardness changes of less than 600 MPa, or yield strength changes of less than 200 MPa.

(\*) Solution-hardening by alloy elements included, otherwise a two-phase alloy cannot be obtained at room temperature.

(\*\*) Solution-hardening of beta by elements such as vanadium is often compensated in a major way by lattice softening due to metastability of the beta or  $\alpha''$  phase. Thus, the extent of solution-hardening cannot be assessed.

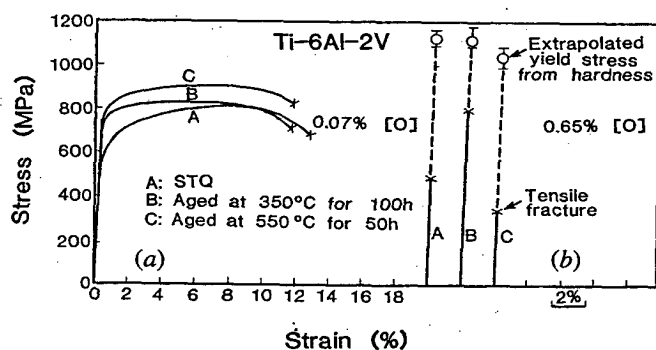


Fig. 13—Tensile stress-strain curves of alpha Ti-6Al-2V alloys in quenched (STQ) and aged conditions. (a) The specimens with low oxygen concentration have good ductility for all heat-treatment conditions. (b) The specimens with high oxygen concentration fractured brittly before the yield stress was reached, regardless of heat-treatment condition. The yield strengths of the brittle tensile samples can be estimated from hardness data (cf. Fig. 14), and are indicated in (b) for the purpose of comparison.

show similar ductilities for the STQ and the aged conditions, with the STQ condition being softest and having the highest ductility. Although the hardness results of the alpha alloy were unaffected by heat treatment (Figure 10), the more

sensitive tensile tests reveal yield strength increases by as much as 22 pct. This increase may be due to Ti<sub>3</sub>Al precipitation (Figure 5) and/or oxygen rearrangement. An important result of Figure 13(a) is that the ductility of alpha is not sensitive to heat treatment. Oxygen, however, severely embrittles the alpha alloy (Figure 13(b)).

The yield strength of the alloys with 0.65 pct oxygen could not be measured directly because the samples failed in a brittle manner before yielding was reached. An estimate of the tensile yield strengths of the brittle samples may be obtained from the hardness data. A linear relation between hardness and yield strength is often assumed with a proportionality factor of about 3,<sup>62,78,79</sup> except for materials whose work-hardenability is appreciable. Better, an extrapolation of measured yield strength vs hardness data can be used, as in Figure 14, to infer the tensile yield strengths of the specimens with hardness of greater than 3500 MPa. The inferred yield strengths are also shown in Figure 13 for comparison.

2. *Beta Alloy:* The tensile behavior is very different from that of the alpha alloy. In the STQ condition the alloy with the lowest oxygen concentration (0.13 pct) is very soft. Its yield strength is only 311 MPa, and it has high ductility with an elongation of 32 pct in a 25 mm gage length (Figure 15(a)). Higher oxygen concentration (0.59 wt pct)

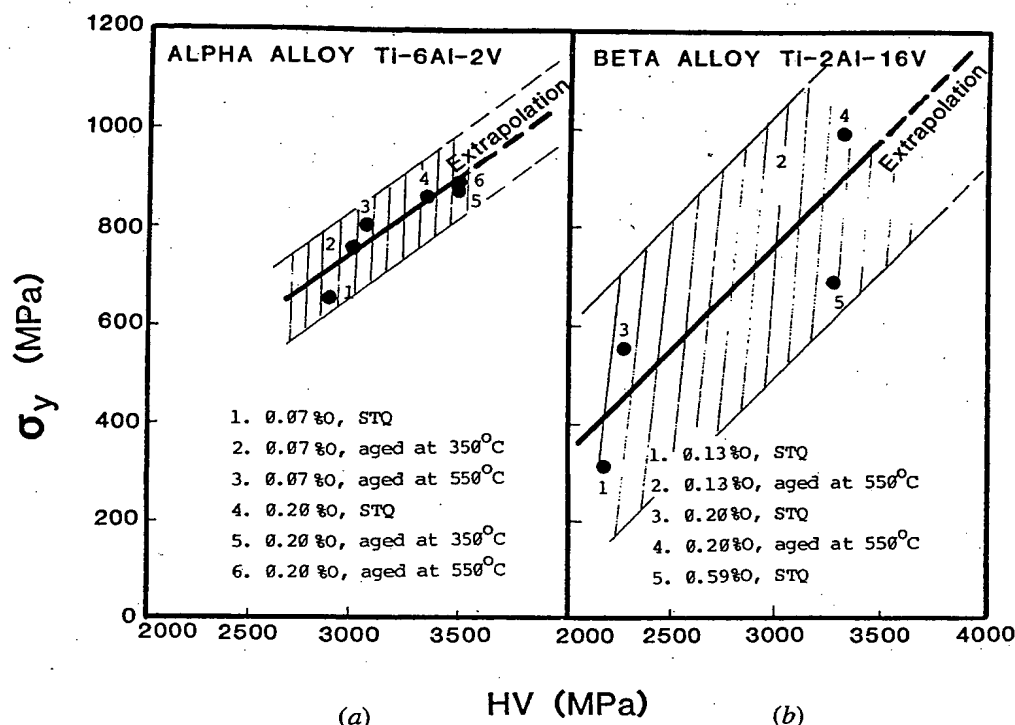


Fig. 14—Relations between Vickers hardness and yield strength for (a) alpha alloy, (b) beta alloy. The extrapolations of the linear regression lines were used to infer yield strengths of those samples which failed brittly in tension.

produces increased yield strength (690 MPa) and reduced ductility of about 5 pct elongation (Figure 15(d)). But it does not embrittle the beta alloy. Aging, on the other hand, not only strengthens the alloy, but also reduces its ductility to very small values (curves b, c, e, and f in Figure 15). Because of brittle fracture the tensile yield strengths of the aged alloys could not be measured directly. Again, yield strengths inferred from hardness data (Figure 14(b)) are shown in Figure 15 for comparison.

In summary, heat treatment has a large effect on the strength of the beta alloy. The precipitation of alpha (and

to some extent of omega particles) is responsible for the strength increase and for the embrittlement of the aged specimens. Oxygen strengthens beta equally as much as alpha. Oxygen in high concentration reduces the ductility of beta but not to the extent of embrittlement.

#### F. Fracture Surface

1. *Alpha Alloy*: Characterization of tensile rupture surfaces by SEM confirmed the ductile fracture mode of the alpha alloy with 0.07 pct oxygen. A cellular dimple struc-

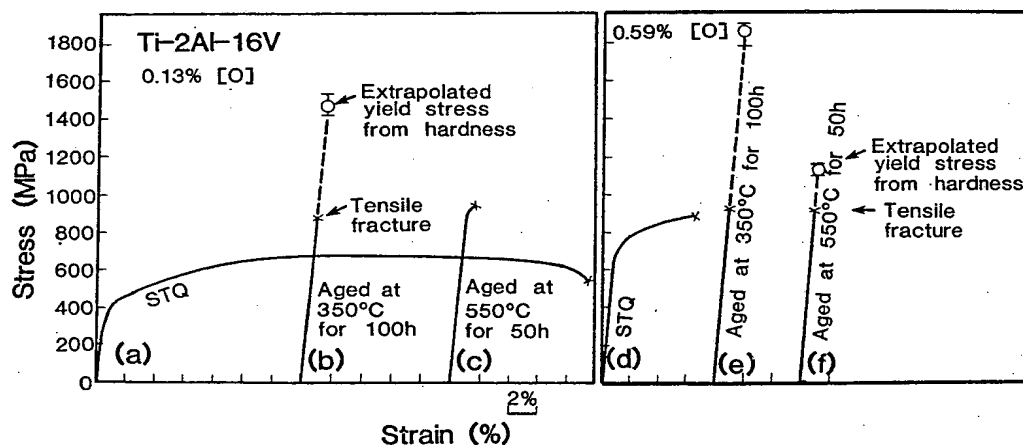


Fig. 15—Tensile stress-strain curves of beta Ti-2Al-16V alloys in quenched (STQ) and aged conditions. In the STQ condition both the low-oxygen and the high-oxygen alloys are ductile. The extremely low yield strength (Y.S.) of the quenched alloy with 0.13 wt pct [O], is due to metastable  $\beta/\alpha''$  phases.<sup>16</sup> In the aged conditions the specimens generally fractured (indicated by x) before macroscopic yielding occurred. The yield strengths of these samples were inferred from hardness data (cf. Fig. 14), and are shown for comparison.

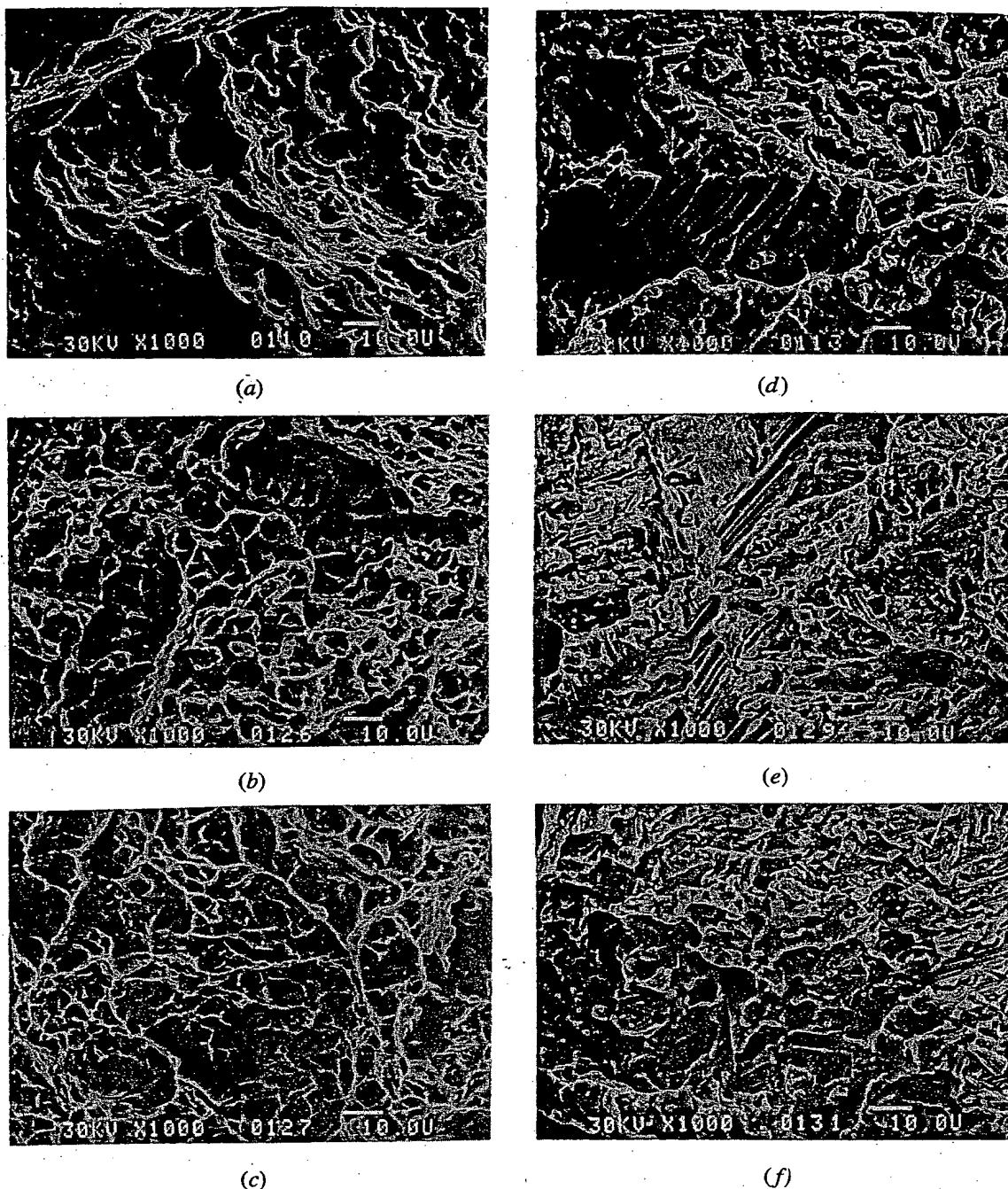


Fig. 16—SEM fractographs of alpha alloys, Ti-6Al-2V, ruptured in tension at room temperature. (a) 0.07 pct [O], STQ, ductile, (b) 0.07 pct [O], aged at 350 °C for 100 h, ductile, (c) 0.07 pct [O], aged at 550 °C for 50 h, ductile, (d) 0.65 pct [O], STQ, brittle, (e) 0.65 pct [O], aged at 350 °C for 100 h, brittle, and (f) 0.65 pct [O], aged at 550 °C for 50 h, brittle.

ture, characteristic of ductile deformation, appears in the STQ and the aged conditions (Figures 16(a), (b), and (c)). The alpha alloy with 0.65 pct oxygen, on the other hand, fractured in a brittle mode for each of the heat-treatment conditions (Figures 16(d), (e), and (f)). The fracture path appears to be intergranular along lamella boundaries or cleavage across lamellae. There are no signs of plastic deformation.

2. *Beta Alloy*: The tensile rupture surfaces of the beta alloy are shown in Figure 17. In the STQ condition the

fractures are ductile at low and high oxygen concentrations (Figures 16(a) and (d)). The cellular dimple structure is evidence of good ductility. In the aged conditions, however, the fracture mode changed to completely brittle. In the 350 °C-aged alloys the fracture is brittle transgranular (Figures 17(b) and (e)). In the 550 °C-aged alloys the fractures are brittle intergranular with occasional transgranular paths (Figures 17(c) and (f)). Intergranular fracture is believed to be caused by the presence of a layer of alpha precipitates along beta grain boundaries, as observed by optical microscopy and TEM (Figures 8 and 18).

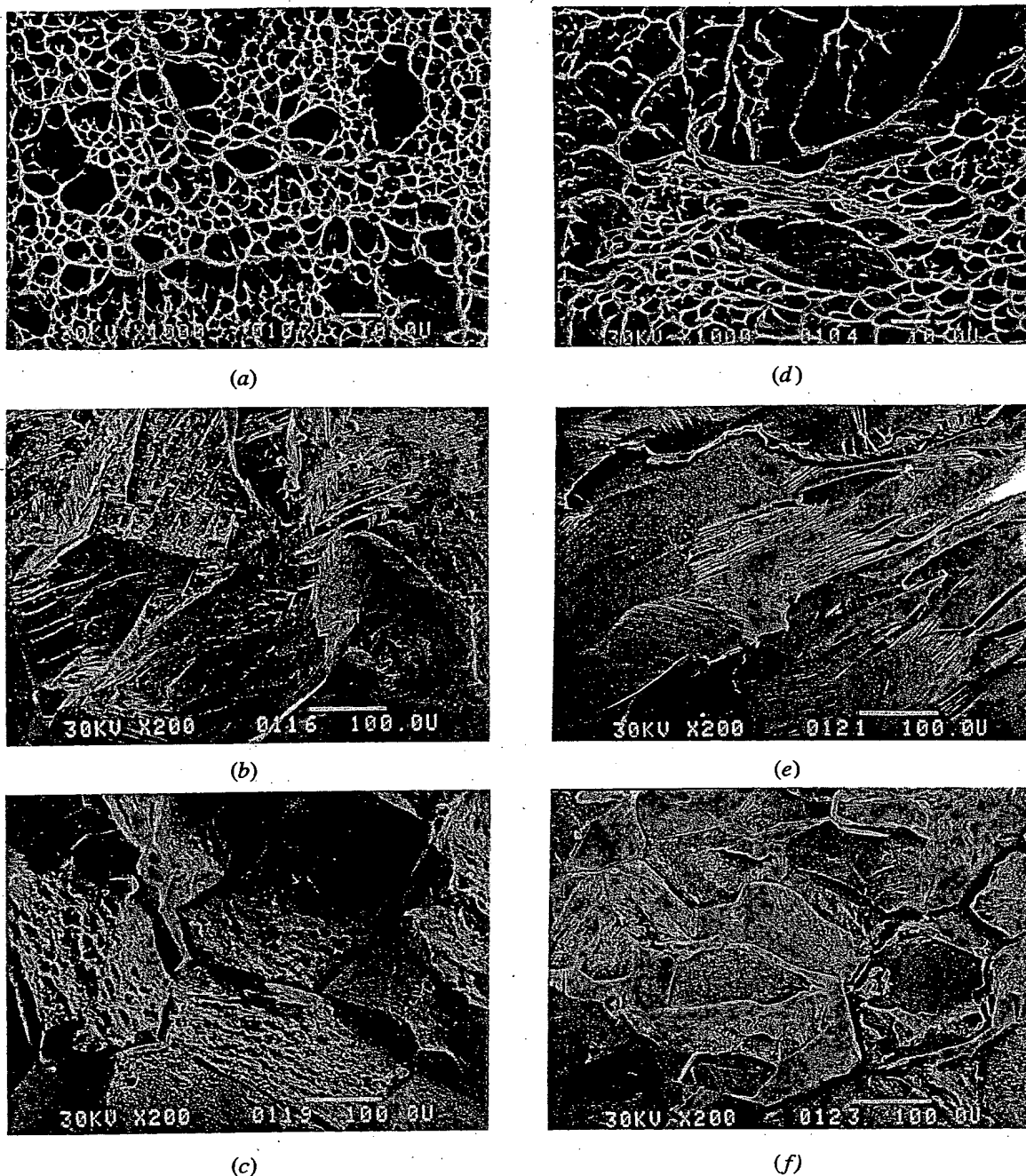


Fig. 17—SEM fractographs of beta alloys, Ti-2Al-16V, ruptured in tension at room temperature. (a) 0.13 pct [O], STQ, ductile, (b) 0.13 pct [O], aged at 350 °C for 100 h, brittle transgranular, (c) 0.13 pct [O], aged at 550 °C for 50 h, brittle intergranular and transgranular, (d) 0.59 pct [O], STQ, ductile, (e) 0.59 pct [O], aged at 350 °C for 100 h, brittle transgranular, and (f) 0.59 pct [O], aged at 550 °C for 50 h, brittle intergranular and transgranular.

#### IV. CONCLUSIONS

Microstructural, diffraction, and mechanical evaluation of separate alpha and beta titanium alloys were conducted to provide a better understanding of the effects of interstitial oxygen and of heat treatment on the strengths and ductilities of these alloys. The effects are summarized below.

##### A. Oxygen Effects

1. Oxygen hardens the alpha and beta alloys to the same degree with a square root dependency on concentration.

The hardening potential of oxygen is little affected by heat treatment.

2. Oxygen at a level of 0.65 wt pct embrittles the alpha alloy. Brittle fracture occurs along lamella boundaries and by cleavage through the lamellae.
3. Although there is no evidence of oxygen ordering from X-ray diffraction, TEM reveals superdislocation pairs in alpha alloy with 0.65 pct oxygen, indicating the existence of oxygen-order. No such superdislocation pairs were found in specimens in which there was diffraction evidence of  $Ti_3Al$ .





Fig. 18—TEM photograph of beta alloy with 0.59 pct oxygen, aged at 550 °C for 50 h. A continuous sheath of alpha precipitates has formed along a grain boundary. This precipitation is believed to be responsible for the brittle intergranular fractures shown in Figs. 17(c) and (f). Small alpha precipitates exist also inside the beta grains. The insert shows a [111]-beta diffraction pattern superposed by several  $\alpha$ -patterns of [2 $\bar{1}$ 10] and [2 $\bar{1}$ 13] zone axes. Compare also with Fig. 8(b).

4. Oxygen enhances  $\text{Ti}_3\text{Al}$  precipitation during aging.
5. The homogeneous beta alloys are metastable at room temperature. In the STQ condition they are mostly in the form of the orthorhombic  $\alpha''$  martensite phase. At high oxygen concentration (0.59 wt pct) the orthorhombic  $\alpha''$  is suppressed in favor of  $\beta$ .
6. Oxygen reduces the ductility of the beta alloy, but it does not embrittle the alloy even at a concentration as high as 0.59 wt pct.

#### B. Aging Effects

1. Aging at 550 °C produces traces of  $\text{Ti}_3\text{Al}$  precipitation in the alpha alloy. Nevertheless, the alpha alloy is only weakly age-hardened. Aging does not embrittle the alpha alloy.
2. Alpha and omega precipitates form during low temperature (350 °C) aging in the beta alloy. At higher aging temperature (550 °C) only alpha precipitates are formed. The precipitates are responsible for strong age-hardenability of the beta alloy.
3. Aging embrittles the beta alloy and causes transgranular fracture after 350 °C aging and mostly intergranular fracture after 550 °C aging. The latter is due to decoration of grain boundaries with alpha precipitates.
4. In the STQ condition the beta alloy is softer than alpha, but after aging the hardness of beta can significantly exceed that of alpha.

The strengths and ductilities of the isolated alpha and beta alloys and the effects of oxygen and heat treatment have been shown to be of direct relevance for the two-phase Ti-6Al-4V alloy. There is good agreement for the dependency of hardness on oxygen level between rule of mixture curves and Ti-6Al-4V data. This agreement holds for several heat-treatment conditions. The microstructural characteristics of the alpha and the beta alloys and their responses to increased oxygen concentration or to aging treatments have been correlated with tensile and hardness properties. These correlations also provide consistent explanations of the property changes of the Ti-6Al-4V alloy.

## ACKNOWLEDGMENTS

This research was supported in part by the National Science Foundation under grant No. 8121772. The alloys were made with support by the Office of Naval Research under grant No. N0001484G0075.

## REFERENCES

1. R. I. Jaffee, H. R. Ogden, and D. J. Maykuth: *Trans. AIME*, 1950, vol. 188, pp. 1261-66.
2. H. Conrad, M. Doner, and B. de Meester: *Titanium Science and Technology*, Plenum Press, 1973, pp. 969-1005.
3. H. Conrad: *Progr. in Mat. Science*, 1981, vol. 26, pp. 123-403.
4. H. Conrad: *Can. J. Phys.*, 1967, vol. 45, pp. 581-90.
5. R. Jaffee: Presentation at TMS-AIME meeting, spring 1987, Denver, CO.
6. R. W. Judy, Jr., B. B. Rath, and R. G. Goode: *Titanium Science and Technology*, DGM, 1985, pp. 1925-43.
7. H. Margolin and J. P. Nielsen: *Modern Materials*, H. H. Hausner, ed., Academic Press, 1960, vol. 2, pp. 291-307.
8. K. S. Chan, C. C. Wojcik, and D. A. Koss: *Metall. Trans. A*, 1981, vol. 12A, pp. 1899-1907.
9. S. Ankem and H. Margolin: *Metall. Trans. A*, 1980, vol. 11A, pp. 963-72.
10. J. C. Williams, A. W. Thompson, C. G. Rhodes, and J. C. Chesnutt: *Titanium and Titanium Alloys*, Plenum Press, 1976, pp. 467-96.
11. I. W. Hall and C. Hammond: *Titanium and Titanium Alloys*, Plenum Press, 1976, pp. 601-14.
12. M. Peters and J. C. Williams: *Titanium Science and Technology*, DGM, 1985, pp. 1843-50.
13. G. Welsch, G. Lütjering, K. Gazioglu, and W. Bunk: *Metall. Trans. A*, 1977, vol. 8A, pp. 169-77.
14. G. Welsch and W. Bunk: *Metall. Trans. A*, 1982, vol. 13A, pp. 889-99.
15. T. W. Duerig, R. M. Middleton, G. T. Terlinde, and J. C. Williams: *Titanium '80 Science and Technology*, TMS-AIME, 1980, vol. 2, pp. 1503-12.
16. Y. T. Lee and G. Welsch: *Titanium Science and Technology*, DGM, 1985, pp. 1689-96.
17. Y. T. Lee: Ph.D. Thesis, Case Western Reserve University, Cleveland, OH, 1985.
18. G. Welsch and M. Weller: in *Role of Interfaces in Material Damping*, B. B. Rath and M. S. Misra, eds., ASM, 1985, pp. 73-78.
19. A. Lasalmonie and M. Loubardou: *J. Mat. Sci.*, 1979, vol. 14, pp. 2589-95.
20. Y. Murakami, O. Izumi, and T. Nishimura: *Titanium Science and Technology*, DGM, 1985, vol. 3, pp. 1403-22.
21. M. A. Imam, B. B. Rath, and D. J. Gillespie: *Titanium Science and Technology*, DGM, 1985, vol. 3, pp. 1511-18.
22. H. Y. Yu, M. A. Imam, and B. B. Rath: *Titanium Science and Technology*, DGM, 1985, vol. 3, pp. 1819-26.
23. H. Becker: *Z. Metall.*, 1981, vol. 72, pp. 679-87.
24. T. W. Duerig, G. T. Terlinde, and J. C. Williams: *Metall. Trans. A*, 1980, vol. 11A, pp. 1987-98.
25. G. T. Terlinde, T. W. Duerig, and J. C. Williams: *Metall. Trans. A*, 1983, vol. 14A, pp. 2101-15.
26. G. H. Isaac and C. Hammond: *Titanium Science and Technology*, DGM, 1985, vol. 3, pp. 1535-42.
27. Y. Murakami, K. Nakao, Y. Yasuda, N. Tokushige, H. Yoshida, and Y. Moriguchi: *Titanium Science and Technology*, DGM, 1985, vol. 3, pp. 1543-50.
28. H. M. Flower, A. I. P. Nwobu, and D. R. F. West: *Titanium Science and Technology*, DGM, 1985, vol. 3, pp. 1567-74.
29. T. Sugitomo, K. Kamei, S. Komatsu, K. Sugimoto, H. Matsumoto, and M. Ikeda: *Titanium Science and Technology*, DGM, 1985, vol. 3, pp. 1583-90.
30. R. Castro and L. Seraphin: *Mem. Sci. Rev. Met.*, 1966, vol. 63, pp. 1025-58.
31. R. E. Curtis and W. F. Spurr: *Trans. ASM*, 1968, vol. 61, pp. 115-27.
32. S. Naka: Ph.D. Thesis, University of South Paris, 1983.
33. M. Majdic, G. Welsch, and G. Ziegler: *Titanium and Titanium Alloys*, Plenum Press, 1976, pp. 1905-18.
34. A. I. Kahveci and G. Welsch: *Scripta Metall.*, 1986, vol. 20, pp. 1287-90.

35. Z. Liu and G. Welsch: Case Western Reserve University, Cleveland, OH, unpublished research, 1987.
36. F. Larson and A. Zarkades: MCIC Report No. MCIC-74-20, 1974.
37. S. Yamaguchi: *J. Phys. Soc. Jpn.*, 1969, vol. 27, pp. 155-63.
38. T. K. G. Nambodhiri, C. J. McMahon, Jr., and H. Herman: *Metall. Trans.*, 1973, vol. 4, pp. 1323-31.
39. D. J. Truax and C. J. McMahon, Jr.: *Mat. Sci. Eng.*, 1974, vol. 13, pp. 125-39.
40. P. C. Gehlen: *The Science, Technology and Application of Titanium*, Pergamon Press, 1968, pp. 349-57.
41. J. Y. Lim, C. J. McMahon, Jr., D. P. Pope, and J. C. Williams: *Metall. Trans. A*, 1976, vol. 7A, pp. 139-44.
42. R. M. Middleton and C. R. Hickey, Jr.: *Titanium and Titanium Alloys*, Plenum Press, 1976, pp. 1567-81.
43. N. A. Nikhanorov and V. V. Latsh: *Titanium and Titanium Alloys*, Plenum Press, 1976, pp. 1651-60.
44. N. E. Paton and J. C. Williams: *Scripta Metall.*, 1973, vol. 7, pp. 647-50.
45. A. I. Kahveci: Ph.D. Thesis, Case Western Reserve University, Cleveland, OH, 1988.
46. J. C. Williams and M. J. Blackburn: *Trans. ASM*, 1967, vol. 60, pp. 373-83.
47. P. J. Fopiano and C. F. Hickey, Jr.: *The Science, Technology and Application of Titanium*, Pergamon Press, 1970, pp. 815-16.
48. H. Gegel: *op. cit.* 75 in H. Conrad, M. Doner, and B. de Meester, *Titanium Science and Technology*, Plenum Press, 1973, pp. 969-1008.
49. H. Sasano and H. Kimura: *Titanium '80 Science and Technology*, TMS-AIME, 1980, pp. 1147-54.
50. I. Weiss, G. Welsch, F. H. Froes, and D. Eylon: *Strength of Metals and Alloys*, Pergamon Press, 1985, vol. 2, pp. 1073-78.
51. H. W. Rosenberg: *The Science, Technology and Application of Titanium*, Pergamon Press, 1970, pp. 851-59.
52. K. Shimasaki, K. Ono, and T. Tsuruno: *Titanium '80 Science and Technology*, TMS-AIME, 1980, vol. 2, pp. 1131-35.
53. P. J. Fopiano, M. B. Bever, and B. L. Averbach: *Trans. ASM*, 1969, vol. 62, pp. 324-32.
54. J. D. Boyd and R. G. Hoagland: *Titanium Science and Technology*, Plenum Press, 1973, vol. 2, pp. 1071-83.
55. M. Peters, K. Welpmann, and H. Döcker: *Titanium Science and Technology*, DGM, 1985, vol. 4, pp. 2267-74.
56. K. Okazaki and H. Conrad: *Acta Metall.*, 1973, vol. 21, pp. 1117-29.
57. H. Conrad and R. Jones: *The Science, Technology and Application of Titanium*, Pergamon Press, 1970, pp. 489-501.
58. I. Weiss, F. H. Froes, and P. J. Bania: *Strength of Metals and Alloys*, Pergamon Press, 1985, vol. 2, pp. 1055-66.
59. W. -B. Busch and H. -D. Kunze: *Titanium Science and Technology*, DGM, 1985, vol. 2, pp. 725-32.
60. S. N. Monteiro, A. T. Santhanam, and R. E. Reed-Hill: *The Science, Technology and Application of Titanium*, Pergamon Press, 1970, pp. 503-16.
61. L. W. Meyer: *Titanium Science and Technology*, DGM, 1985, vol. 2, pp. 1851-58.
62. M. F. Ashby and D. R. H. Jones: *Engineering Materials*, Pergamon Press, 1982, p. 106.
63. E. W. Collings: *The Physical Metallurgies of Titanium Alloys*, ASM, 1984, pp. 115-22.
64. L. E. Tanner, A. R. Pelton, and R. Gronski: *J. de Physique*, 1974, vol. 43, pp. C4-169.
65. D. A. Koss: The Pennsylvania State University, PA, private communication, 1987.
66. Z. Liu: Ph.D. Thesis, Case Western Reserve University, Cleveland, OH, 1988.
67. D. Eylon and C. M. Pierce: *Metall. Trans. A*, 1976, vol. 7, pp. 111-21.
68. S. L. Semiatin and G. D. Lahoti: *Metall. Trans. A*, 1981, vol. 12, pp. 1705-17.
69. H. Margolin and P. Cohen: *Titanium '80 Science and Technology*, AIME, 1980, pp. 1555-61.
70. A. Gogia, D. Banerjee, and N. C. Birla: *Trans. Indian Inst. Met.*, 1983, vol. 36, pp. 200-07.
71. I. Weiss, F. H. Froes, D. Eylon, and G. Welsch: *Metall. Trans. A*, 1986, vol. 17A, pp. 1935-47.
72. S. M. L. Sastry, T. C. Peng, and J. E. O'Neal: *Titanium Science and Technology*, DGM, 1985, vol. 3, pp. 1811-18.
73. G. R. Yoder, L. A. Cooley, and T. W. Crooker: *Titanium '80 Science and Technology*, AIME, 1980, vol. 3, pp. 1865-73.
74. J. C. Chesnutt, A. W. Thompson, and J. C. Williams: *Titanium Science and Technology*, AIME, 1980, vol. 3, pp. 1875-82.
75. G. Lütjering and A. Gysler: *Titanium Science and Technology*, DGM, 1985, vol. 4, pp. 2065-83.
76. L. Levin, R. G. Vogt, D. Eylon, and F. H. Froes: *Titanium Science and Technology*, DGM, 1985, vol. 4, pp. 2107-14.
77. D. S. Shih, F. S. Lin, and E. A. Starke: *Titanium Science and Technology*, DGM, 1985, vol. 4, pp. 2259-66.
78. M. J. Blackburn and J. C. Williams: *Trans. ASM*, 1969, vol. 62, pp. 298-409.
79. D. Tabor: *The Hardness of Metal*, Oxford, Clarendon Press, 1951, p. 106.